



Universidad Autónoma  
de Madrid

**Biblos-e Archivo**  
Repositorio Institucional UAM

**Repositorio Institucional de la Universidad Autónoma de Madrid**

<https://repositorio.uam.es>

Esta es la **versión de autor** del artículo publicado en:  
This is an **author produced version** of a paper published in:

Environmental Science: Nano 6.5 (2019): 1382-1392

**DOI:** <https://doi.org/10.1039/c8en01427b>

**Copyright:** © 2019 The Royal Society of Chemistry

El acceso a la versión del editor puede requerir la suscripción del recurso

Access to the published version may require subscription

# Secondary nanoplastics released from a biodegradable microplastic severely impact freshwater environments

Miguel González-Pleiter<sup>1,\*</sup>, Miguel Tamayo-Belda<sup>1</sup>, Gerardo Pulido-Reyes<sup>1</sup>, Georgiana Amariei<sup>2</sup>, Francisco Leganés<sup>1</sup>, Roberto Rosal<sup>2</sup> and Francisca Fernández-Piñas<sup>1</sup>

<sup>1</sup> Department of Biology, Faculty of Science, Universidad Autónoma de Madrid, Spain

<sup>2</sup> Department of Chemical Engineering, Universidad de Alcalá, E-28871 Alcalá de Henares, Spain

\* Corresponding author: mig.gonzalez@uam.es

## Abstract

Over the last five decades, plastics production has increased because of their use in strategic sectors causing damage on aquatic ecosystems. In this context, biodegradable plastics have emerged as an ecological alternative because they are easily degradable in the environment. Despite the recent advances in the field of plastic ecotoxicology, the ecological impact of secondary nanoplastics (nanoplastics resulting from natural degradation of micro and macro plastics) in the environment remains poorly understood. Here, we have investigated the effects of secondary nanoplastics of polyhydroxybutyrate (PHB), a biodegradable plastic, on three representative organisms of aquatic ecosystems. Secondary PHB-nanoplastics were produced from PHB-microplastics by abiotic degradation under environmentally representative conditions. Secondary PHB-nanoplastics induced a significant decrease in cellular growth and altered relevant physiological parameters in all organisms. We investigated whether the observed toxicity was exerted by PHB-nanoplastics themselves or by other abiotic degradation products released from PHB-microplastics. An experiment was run in which PHB-nanoplastics were removed by ultrafiltration; the resulting supernatant was not toxic to the organisms, ruling out the presence of toxic chemicals in the PHB-microplastics. In addition, we have performed a complete physicochemical characterization confirming the presence of secondary PHB-nanoplastics in the 75–200 nm range. All results put together indicated that secondary PHB-nanoplastics released because of the abiotic degradation of PHB-microplastics were harmful for the tested organisms, suggesting that biodegradable plastic does not mean safe for the environment in the case of PHB.

## Introduction

Plastics are polymers (small molecules -monomers- linked together in a repetitive formation) made up of carbon, hydrogen, oxygen, nitrogen, silicon and chloride, which may also contain additives to improve physical properties and/or reduce costs <sup>1-4</sup>. Over the last five decades, plastics production has increased due to their use in strategic sectors such as packaging, construction, automotive, electronic, household, leisure and sports, agriculture, renewable energy or medical devices <sup>5, 6</sup>. Excluding fibers, almost 348 million tons of plastics have been produced around the world only in 2018 <sup>5</sup> and almost 6% of the fossil resource extracted in the world are currently used to their manufacture. The main advantages of plastics are their light-weight, inertness, durability, strength and low cost. On the other hand, their high molecular weight, complex three-dimensional structure and hydrophobic nature hinder their degradation, making them recalcitrant compounds that accumulate in enormous quantities in the environment <sup>4</sup>. In this context, biodegradable plastics are considered the best candidates to replace non-biodegradable plastics<sup>1</sup>. By definition,

they are plastics that can be recognized by enzymes present in nature independently of whether their source is renewable or fossil <sup>6</sup>. Among them, polyhydroxybutyrate (PHB), a melt-processable semi-crystalline polyester synthesized by many microorganisms from renewable resources (in contrast with other biodegradable plastics), has received special attention due to their great thermal and ultraviolet resistance and water insoluble. Currently, PHB is widely used for biomedical applications <sup>7</sup>.

Due to their widespread use, plastics end up into the aquatic environments. The major pathways of entry in the freshwater compartment are wastewater treatment plants (WWTPs) and atmospheric deposition (i.e., plastics transported by wind) <sup>8, 9</sup>. For the marine environment, land sources contribute to 80% of the plastic debris, highlighting the key role of the freshwater system in the life cycle of plastics <sup>8, 9</sup>. Once plastics reach the environment, they may be susceptible to fragmentation and degradation via abiotic and/or biotic processes <sup>2, 10</sup>. Although there are several abiotic degradation processes such as hydrolytic,

mechanical, thermal and oxidative degradation<sup>10, 11</sup>, it is generally considered that photodegradation is the most efficient abiotic degradation route for plastics<sup>2</sup>. Visible and ultraviolet radiation absorbed by plastics activate their electrons to higher reactivity, promoting their oxidation, cleavage and causing chain scission and cross-linking reactions<sup>11</sup>. Abiotic degradation results in the loss of structural and mechanical properties, creating surface irregularities that facilitate microbial colonization and altering the physicochemical characteristics of the polymer surface<sup>12</sup>. Biotic processes include the secretion of extracellular enzymes that generate oligomers and monomers which can be mineralized by several microorganisms<sup>11, 13</sup>.

During all these abiotic and biotic degradation processes, plastics are converted into smaller particles, the so-called microplastics: plastic particles smaller than 5 mm<sup>14</sup>. Microplastic concentration in freshwater varies depend on sampling locations from 0 to  $1.87 \times 10^5$  microplastics per m<sup>3</sup>. The WWTPs constitute the main source of microplastics to the environment, releasing 8–13 billion microplastics per day<sup>15</sup>. It has been suggested that microplastics will subsequently degrade into plastics in the nano-range (< 1000 nm in one dimension)<sup>3</sup>, the so-called nanoplastics. Nanoplastics can be classified into two different groups according to their sources. The term primary nanoplastic refers to nanoplastics that are manufactured as those contained in personal care products. This differs from secondary nanoplastics, which are the result from fragmentation and degradation processes of macro and microplastic into nanosized particles. It has been reported the formation of secondary nanoplastic particles during the degradation of macro and microplastics based on latex and polystyrene (PS) under laboratory conditions as well as from biodegradable plastic mixture of polylactic acid (PLA) and polyethylene terephthalate (PET) under representative environmental conditions<sup>16–19</sup>. However, it is unknown whether these secondary nanoplastics are being produced and accumulated in the environment; there are not reliable and appropriate methods for their detection in real samples<sup>10, 16</sup> and only indirect evidence of their presence has been previously shown<sup>17, 18</sup>. In addition to the degradation processes from higher plastics, nanoplastics could also be introduced into aquatic environment as primary nanoplastics<sup>20</sup>.

There is a rapidly growing body of evidence on the negative effects of primary nanoplastics, especially

on marine organisms. Several manufactured nanoplastics such as polystyrene (PS), polycarbonate (PC), poly(methyl methacrylate) (PMMA) and latex have induced a variety of effects on growth, development, behavior, reproduction and mortality in different organisms such as algae, filter feeders and fish<sup>2, 10, 21, 22</sup>. Trophic transfers of nanoplastics have been also investigated by several authors<sup>2, 10, 21</sup>. However, all these studies are limited to primary nanoplastic specifically synthesized in the laboratory, whereas the effect of secondary nanoplastics produced by degradation processes has not been assessed. Besides, the use of non-biodegradable plastics has prevailed in toxicological experiments, so the effects of biodegradable nanoplastics towards aquatic organisms is completely unknown.

In this work, we investigated the biological effect of secondary PHB-nanoplastics released from PHB-microplastics by abiotic degradation under environmentally representative conditions to three freshwater organisms, the filamentous cyanobacterium *Anabaena* sp. PCC7120, the green alga *Chlamydomonas reinhardtii* Dangeard (strain CCAP 11/32A mt<sup>+</sup>) and the small crustacean *Daphnia magna*. Cyanobacteria and green algae are a fundamental part of the phytoplankton, organisms at the base of the trophic chain in freshwaters, and the crustacean plays a key role as primary consumer in freshwater ecosystems. Therefore, any deleterious effect on them may cause severe damage to higher trophic level organisms, disrupting the ecological balance in the freshwater environment.

## Experimental

### Chemicals

Microplastics (cylinders, 5 mm height, 3 mm diameter, density 1.25 g/cm<sup>3</sup>, apparent density  $1.13 \pm 0.05$  g/cm<sup>3</sup>) of polyhydroxybutyrate (PHB) (> 98%) were obtained from Goodfellow Cambridge Ltd. (Huntingdon, England). PHB was produced by bacterial fermentation and its main impurity was debris of bacterial cell wall. Their crystallinity was 50% obtained by Differential Scanning Calorimetry (DSC) in a TA Instruments Q100 apparatus. Ultrapure water was generated using a Direct-Q™ 5 Ultrapure Water Systems from Millipore (Bedford, MA, USA) with a specific resistance of 18.2 MΩ cm at 25°C.

### Formation of secondary nanoplastics

The release of PHB-nanoplastics from PHB-microplastics was performed as follows: different initial concentrations of PHB-microplastics (25, 50

and 100 mg/L) were immersed in 20 mL sterilized Milli-Q water buffered with 2 mM of phosphate (pH 7.0) placed into 50 mL Erlenmeyer flasks in a room at 28 °C under constant shaking (135 rpm) and irradiation (ca. 65  $\mu\text{mol photons m}^{-2} \text{s}^{-1}$ ; Philips Master TL-D 90 De Luxe 36W/965) during 3 days (Fig. 1A). The conditions simulate solar irradiation in the visible range, which are conditions that can be found in nature<sup>23</sup>. For the case of kinetic studies and scanning electron microscopy (SEM)

analyses, the abiotic degradation time was increased to 20 days (Fig 1A). Ultrafiltration process was carried out using Vivaspin 20 mL centrifugal concentrators with 50 kDa MWCO ultrafilter (Sartorius AG, Goettingen, Germany), which were carefully washed several times with Milli-Q water before being used. We used a control without plastics. This control was Milli-Q water buffered with 2 mM of phosphate at pH 7.0 exposed to the same experimental conditions.

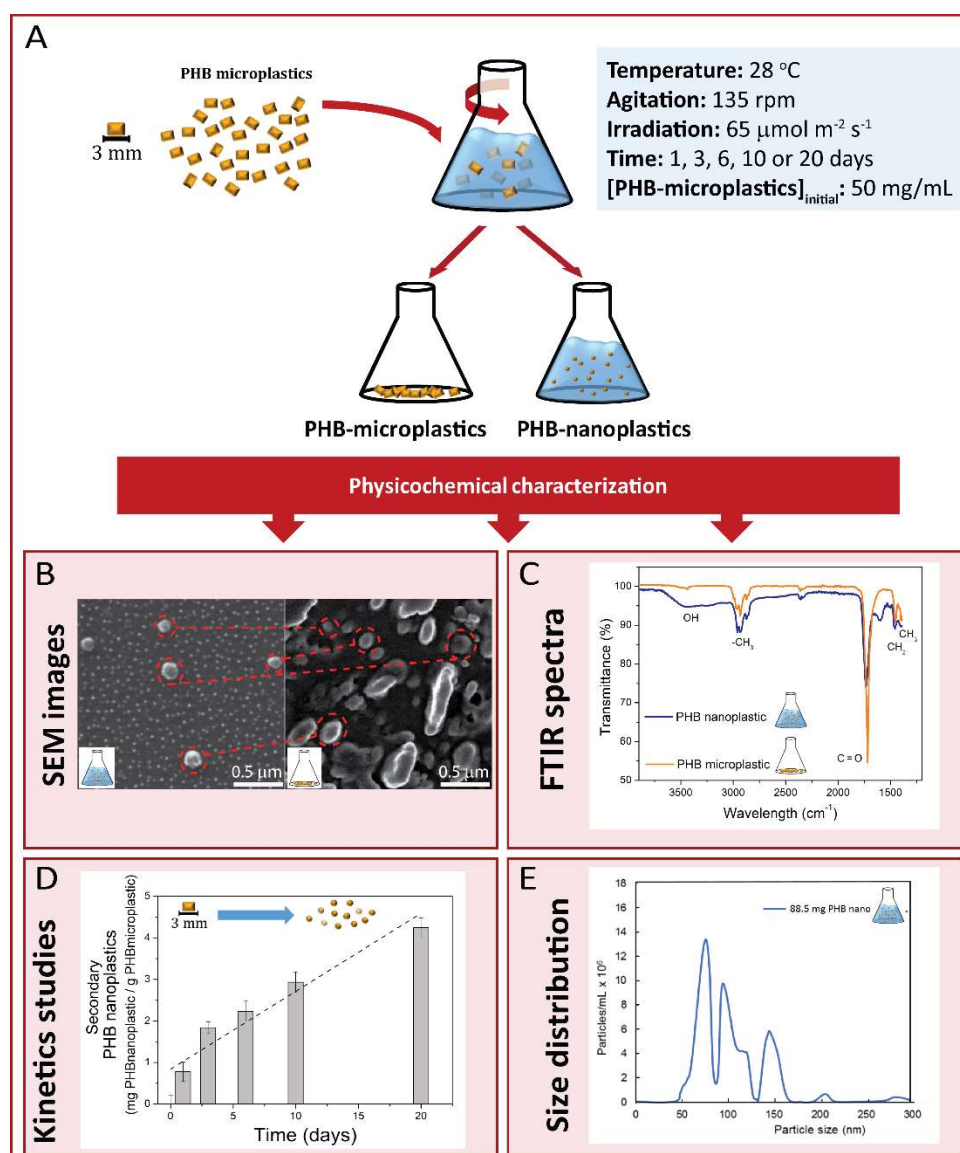


**Figure 1.** Experimental framework explaining the abiotic degradation to obtain secondary PHB-nanoplastics and their physicochemical characterization. A) The experimental scheme of abiotic degradation of PHB-microplastics (50 mg/mL), which release secondary PHB-nanoplastics, and the experimental conditions. B) Scanning electron microscope (SEM) images, on the left, secondary PHB-nanoplastics (free in suspension) released from PHB microplastic after 3 days of abiotic degradation under the conditions described and, on the right, similar particles attached on the surface of PHB-microplastics. C) Attenuated Total Reflectance Fourier Transform Infrared (ATR-FTIR) spectra after of PHB-microplastics and secondary PHB-nanoplastics released from PHB-microplastics after 3 days of abiotic degradation under the conditions described. D) The amount of secondary PHB-nanoplastics per g of PHB-microplastic released as a function of abiotic degradation time. E) Nanoparticle Tracking Analyses (NTA) size distribution of secondary PHB-nanoplastics released from PHB-microplastics after 3 days of abiotic degradation under the described conditions. Milli-Q blank signal was subtracted from the samples.

## Concentration of secondary nanoplastics

The concentration of released PHB-nanoplastics was studied using different initial concentration of PHB-microplastics (25, 50 and 100 mg/L) and times (1, 3, 7, 10 and 20 days), as described above (section: “Secondary PHB-nanoplastics formation”). Concentration of PHB-nanoplastics was calculated from total organic carbon (TOC). Despising the functional groups that could appear after the production of PHB-nanoplastics from PHB-microplastics, a simple calculation using the ratio of C per PHB molecule (0.558 mg TOC/ mg PHB) allowed estimating the mg PHB-nanoplastics per g PHB-microplastics (see details in the Table S1 in the ESI). Total Organic Carbon (TOC) was measured as NPOC (Non-Purgeable Organic Carbon) using a Shimadzu, TOC-VCSH analyser equipped with ASI-V autosampler. The injection volume was 500  $\mu$ L and the autosampler ASI-V typically used 9 mL sample volume including washing procedure and multiple injection points. In NPOC procedure there is no inorganic carbon. This method is the same as TOC but uses sample acidification and sparging for IC removal. Milli-Q water buffered with 2 mM of phosphate at pH 7.0 without plastics exposed to same experimental conditions was used as control. The TOC concentrations of the control at the beginning and at the end of the experiment were  $0.76 \pm 0.01$  mg/L and  $1.93 \pm 0.07$  mg/L, respectively. These values did not result in any significant contribution ( $< 1\%$ ) to the TOC concentration of abiotic experiments with plastics.

## Scanning electron microscopy (SEM)

The morphological characterization of micro and nanoplastics of PHB was performed using SEM. For the SEM images of the nanoplastics, the abiotic degradation process was carried out as described above (section: “Secondary PHB-nanoplastics formation”); thus, 50 mg/mL of PHB microplastics were placed in 20 mL of Milli-Q water buffered with 2 mM phosphate (pH 7.0) at 28 °C in constant shaking for 3 days. Then, 5 mL of supernatant containing PHB-nanoplastics were concentrated 100-fold (from 5 mL to 50  $\mu$ L) during 1 day at room temperature in a laminar flow hood. Concentrated sample was dripped and subsequently dried 5 times over a glass slide. Milli-Q water buffered with 2 mM of phosphate at pH 7.0 without plastics exposed to same experimental conditions was used as control. For the SEM images of the microplastics, 50 mg/mL of PHB-microplastic were abiotically degraded as previously mentioned and three PHB-microplastics were dried after 0, 3 and 20 days of incubation. All samples were metallized with a gold layer of 3 nm using a metallizer Polaron model SC7640 and observed with a SEM Zeiss DSM 950.

## FTIR

Attenuated Total Reflectance Fourier Transform Infrared (ATR-FTIR) spectra of microplastics (0 and 3 days) and nanoplastics (3 days) were obtained using a Thermo-Scientific Nicolet iS10 equipped with a Smart iTR-Diamond ATR module instrument. The spectra were taken in the 4000–500  $\text{cm}^{-1}$  range with a resolution of 4  $\text{cm}^{-1}$ . For the FTIR analysis, the abiotic degradation process was carried out in the same way than that performed for the SEM images. Each measurement was obtained from 64 FTIR scans.

## DLS, NTA and $\zeta$ -potential

Dynamic Light Scattering (DLS) and  $\zeta$ -potential measurements were done with a Zetasizer Nano ZS (Malvern Instruments, Malvern, UK) after 3 days of abiotic degradation from three different initial concentrations of microplastics (25, 50 and 100 mg/L). Nanoparticle Tracking Analyses (NTA) of PHB-nanoplastics produced from PHB-microplastic (25, 50 and 100 mg/L) after 3 days of incubation were performed using a NanoSight NS300 (Malvern Instruments, Malvern, UK) equipped with a 488 nm laser. NanoSight software version NTA 3.2 was used for data accumulation and analysis. Data was recorded using a sCMOS camera using 1498 frames at 25 fps. The Stokes–Einstein equation was used to calculate the mean hydrodynamic diameter. Five video measurements were conducted for each sample to provide an average size and standard deviation.

## Bioassays

Toxicity assays using *Anabaena* sp. PCC7120 (hereinafter, *Anabaena*) and *Chlamydomonas reinhardtii* Dangeard (strain CCAP 11/32A mt<sup>+</sup>) (hereinafter, *C. reinhardtii*) were conducted following the procedure described by Gonzalo et al.<sup>24</sup> and Rosal et al.<sup>25</sup> with minor modifications. They were routinely grown in the light ca. 65  $\mu\text{mol photons m}^{-2} \text{ s}^{-1}$ , at 28 °C, on a rotary shaker (135 rpm) in 100 mL in 250 mL Erlenmeyer flask for 3 days. *Anabaena* was grown in sterile Allen & Arnon culture medium diluted eight-fold supplemented with nitrate (5 mM) buffered with 2 mM of 4-(2-hydroxyethyl)-1-piperazineethanesulfonic acid (HEPES) and adjusted to pH 7.8. *C. reinhardtii* was grown in sterile TAP culture medium (pH 7.0). Cultures (grown as described) were centrifuged and resuspended in fresh medium at  $\text{OD}_{750\text{nm}} = 0.2$ . Then, 20 mL of culture were centrifuged and resuspended in 20 mL of culture medium with secondary PHB-nanoplastics, which have been released from 50 mg/mL of PHB-microplastics in appropriate sterile culture medium during 3 days of

incubation in the absence of cells at 28 °C under constant shaking (135 rpm) and irradiation (ca. 65  $\mu\text{mol photons m}^{-2} \text{ s}^{-1}$ ; Philips Master TL-D 90 De Luxe 36W/965). PHB-microplastics were separated from the supernatant containing the nanoplastics by decanting this supernatant (with the PHB-nanoplastics) over the cell pellet whereas PHB-microplastics remain sunk at the bottom of the flask where the abiotic degradation took place.

Therefore, initial optical density at 750 nm of the bioassays was 0.2. Non-treated cells (not exposed to PHB) resuspended in fresh medium and non-treated cells resuspended in medium previously exposed to same experimental conditions were used as controls. Acute immobilization bioassay with *Daphnia magna* (hereinafter *D. magna*) was conducted using a commercially text kit (Daphtoxkit FTM (MicroBioTests Inc., Gent, Belgium)<sup>25</sup>. *D. magna* individuals were added in the culture medium with secondary PHB-nanoplastics, which had been released from 50 mg/mL of PHB-microplastics in appropriate sterile culture medium during 3 days of incubation in the absence of cells at 28 °C under constant shaking (135 rpm) and irradiation (ca. 65  $\mu\text{mol photons m}^{-2} \text{ s}^{-1}$ ; Philips Master TL-D 90 De Luxe 36W/965). Test plates bioassay with *D. magna* neonates was conducted according to the Standard Operational Procedures of Daphtoxkit FTM adding a total number of 5 neonates into each test well and incubating during 48 h in the dark at 20°C. The ultrafiltered suspension denoted as PHB-NPLs-free was also used for the toxicity bioassays. Cellular growth of photosynthetic organisms was measured by tracking the optical density at 750 nm. The neonates of *D. magna* were considered immobilized if they laid on the bottom of the test plate and did not resume swimming within a period of 15 s according to Daphtoxkit FTM standard operating protocol. The EC<sub>50</sub> values were calculated as mg of secondary PHB-nanoplastics per L after 3 days of exposure for photosynthetic organisms and 2 days for crustacean. EC<sub>50</sub> values were calculated by the dose-response package (drc) using R Software, version 3.3.1. The dose-response curves are shown in the Fig. S7.

### Flow cytometry and confocal microscopy

The toxicological mechanism of PHB-nanoplastics was studied by flow cytometry (FC) for photosynthetic organisms and confocal microscopy for *D. magna* using several fluorochromes (Table S2 in the ESI) with the purpose of analysing the following key physiological parameters: intracellular reactive oxygen species (ROS) formation, membrane integrity, cytoplasmic

membrane potential and intracellular pH.

Mitochondrial membrane potential was evaluated for the specific case of the alga and crustacean. FC analyses of *Anabaena* and *C. reinhardtii* cells were performed on a Beckman Coulter Gallios flow cytometer (Beckman Coulter Life Sciences, Indianapolis, United States) fitted with an argon-ion excitation laser (488 nm), a detector of forward scatter (FS), a detector of side scatter (SS) and four fluorescence detectors with four different wavelength intervals: 505–550 nm (FL1), 550–600 nm (FL2), 600–645 nm (FL3) and >645 nm (FL4) according to Prado et al.<sup>26</sup> and Tamayo-Belda et al.<sup>27</sup>, respectively (see details in the Table S2 in the ESI). *D. magna* neonates exposed to secondary PHB-nanoplastics during 48h were collected and incubated, at room temperature and in darkness, with the appropriate fluorochromes (Table S2 in the ESI) which assesses different physiological parameters prior to the analysis by confocal microscopy following Paul et al.<sup>28</sup> (BCECF), Teplova et al.<sup>29</sup> (JC-1 and PI) and Liu et al.<sup>30</sup> (H<sub>2</sub>DCF-DA). All fluorochrome stock solutions were prepared in dimethyl sulfoxide (DMSO) and stored at –20 °C, with the exception of the solution of propidium iodide (PI), which was made in Milli-Q water and stored at 4 °C. Three independent experiments with triplicate samples were carried out for each parameter. For all the cytometric parameters studied here, at least 10<sup>4</sup> gated cells were analysed using Kaluza software version 1.1 (Beckman Coulter).

### Statistical analysis

Means and standard deviation values were calculated for each treatment from three independent replicate experiments. To determine significant differences among test treatments, data were statistically analyzed conducting an overall one-way analysis of variance (ANOVA) using R software. A  $p < 0.05$  or  $p < 0.001$  was considered statistically significant. When significant differences were observed, means were compared using the multiple-range Tukey's HSD test or Dunnett's test.

### Results

#### Physicochemical characterization of abiotic degradation products from PHB-microplastics

Previous studies have shown that the abiotic degradation of plastics results in the release of nanoplastics<sup>16–19</sup>, however less attention has been paid to biodegradable plastics such as PHB. Scanning Electron Microscopy (SEM) was used to study and characterize the abiotic degradation products. SEM photographs revealed the presence of spherical particles

with diameters around 200 nm (Fig. 1B). Similar size and shape of nanoparticles were also observed on the surface of intact PHB-microplastics (Fig. 1B). Increasing the abiotic degradation time (up to 20 days) provokes gradual smoothing of the surface of the PHB-microplastics as shown by the SEM images (Fig. S1 in the ESI; indicated by arrows). This indicates that the surface of the microplastic was altered over time.

In order to determine the chemical nature of the released nanoparticles, Fourier Transform Infrared Spectroscopy (FTIR) was conducted. FTIR spectrum of secondary nanoparticles was compared with the spectrum of intact PHB-microplastics and both spectra are shown in Fig. 1C. The most characteristic band at 1720-1740  $\text{cm}^{-1}$  was assigned to C=O stretching vibration of the carbonyl band, related with the PHB ester group present in the molecular chain of a highly ordered crystalline structure. The peaks at 1452  $\text{cm}^{-1}$  and 1378  $\text{cm}^{-1}$  corresponded to -CH<sub>3</sub> and -CH<sub>2</sub> groups, respectively. The bands at 2900  $\text{cm}^{-1}$  and 3400  $\text{cm}^{-1}$  indicated the presence of alkyl-CH<sub>3</sub> groups and that of the stretching band of hydroxyl terminal -OH group, respectively<sup>31</sup>. Spectra of secondary nanoparticles exhibited the same characteristic absorption bands than intact PHB-microplastics; therefore, FTIR results confirmed that the formed nanoparticles came, originally, from PHB-microplastics. It was also observed that, after 3 days of abiotic degradation, the FTIR spectra of degraded PHB-microplastics (after contact) were the same as those of neat PHB microplastic beads (before contact) (Fig. S2 in the ESI). Given the penetration depth of ATR-FTIR, it was not possible to perform quantitative comparisons, but the main features of PHB backbone were easily recognized, suggesting that PHB depolymerization was taking place at the microplastic surface.

We investigated the kinetics of the secondary PHB-nanoplastics released from PHB-microplastics. Fig. 1D shows that the amount of PHB-nanoplastics increased as a function of abiotic degradation time, thus,  $0.78 \pm 0.24$ ,  $1.8 \pm 0.14$ ,  $2.2 \pm 0.25$ ,  $2.931 \pm 0.25$  and  $4.3 \pm 0.24$  mg secondary PHB-nanoplastics / g PHB-microplastics were found after 1, 3, 6, 10 and 20 days of abiotic degradation, respectively, suggesting a linear relationship of released secondary nanoplastic particles over time. In addition, the amount of secondary PHB-PHB-microplastic exposed to abiotic degradation (Fig. S3 in the ESI). Therefore, the results showed an nanoplastics from different concentrations of PHB was also evaluated. There was also a positive linear relationship between the amount of secondary PHB-nanoplastic released and the initial concentration of increase in the formation of secondary PHB-nanoplastics over time and dependent on initial concentration of PHB-microplastics.

A characterization of the generated secondary PHB-nanoplastics in term of size, particle distribution and surface charge were performed by nanoparticle tracking analysis (NTA), dynamic light scattering (DLS) and  $\zeta$ -potential. As shown in Fig. 1E, the sizes of PHB-nanoplastics calculated by NTA technique were mainly distributed in the 75-200 nm range with a predominant peak at 75 after 3 days in contact with water and after subtracting the water background. DLS measurements also confirmed the presence of PHB-nanoplastics with hydrodynamic sizes around 200 nm (Table S3 in the ESI; Fig. S4B in the ESI). To fully characterize the secondary PHB-nanoplastics released from PHB-microplastics (hereinafter denoted as PHB-NPLs), further analyses of the composition of the PHB-NPLs suspension were performed. The PHB-NPLs suspension was ultrafiltered by a 50 kDa filter (pore size of approximately 4 nm;<sup>32</sup>) and, then, the residual suspension (hereinafter denoted as PHB-NPLs-free) was studied by DLS. No nanoparticles could be measured in the PHB-NPLs-free. The DLS signals of ultrafiltered suspension (Fig. S4C in the ESI) were not different from those of the control: Milli-Q water buffered with 2 mM of phosphate at pH 7.0 (Fig. S4D in the ESI). This indicates that the ultrafiltered suspensions was composed mainly of dissolved matter whereas in the non-ultrafiltered suspension the observed DLS signals corresponded to particulate matter in a colloidal state (Fig. S4A in the ESI). The total number of formed PHB-NPLs per unit mass of PHB-microplastic was inversely proportional to the concentration of initial PHB-microplastics (Fig. S5 in the ESI) because of the higher aggregation when a larger amount of PHB-NPLs passed to the solution (Fig. S6 in the ESI). The obtained nanoparticles were negatively charged with  $\zeta$ -potential  $-19.7 \pm 3.4$  mV at pH 7, indicating a stable colloidal suspension (Table S3 in the ESI). Putting all these results together, abiotic degradation of PHB-microplastics at environmental relevant conditions resulted in the release of PHB-NPLs of 75-200 nm due to a depolymerization process. The hydrolysis of PHB into smaller units is known to start by a random chain scission of ester bonds<sup>33</sup>. The hydrolytic degradation of PHB was shown to proceed faster in amorphous regions, which are more readily accessible to water molecules than PHB crystallites<sup>34</sup>. The degradation of PHB and other polyalkanoates has been shown to progress with molecular weight decrease, weight loss, a general impairment of mechanical properties and, eventually, polymer fragmentation into small fragments<sup>35</sup>. No significant differences ( $p < 0.05$ ) were found between abiotic degradation performed in the dark or under illumination conditions used for the assays (Fig. S7 in the ESI). Therefore, hydrolysis rather than photooxidation could play a key role in the degradation process of PHB.



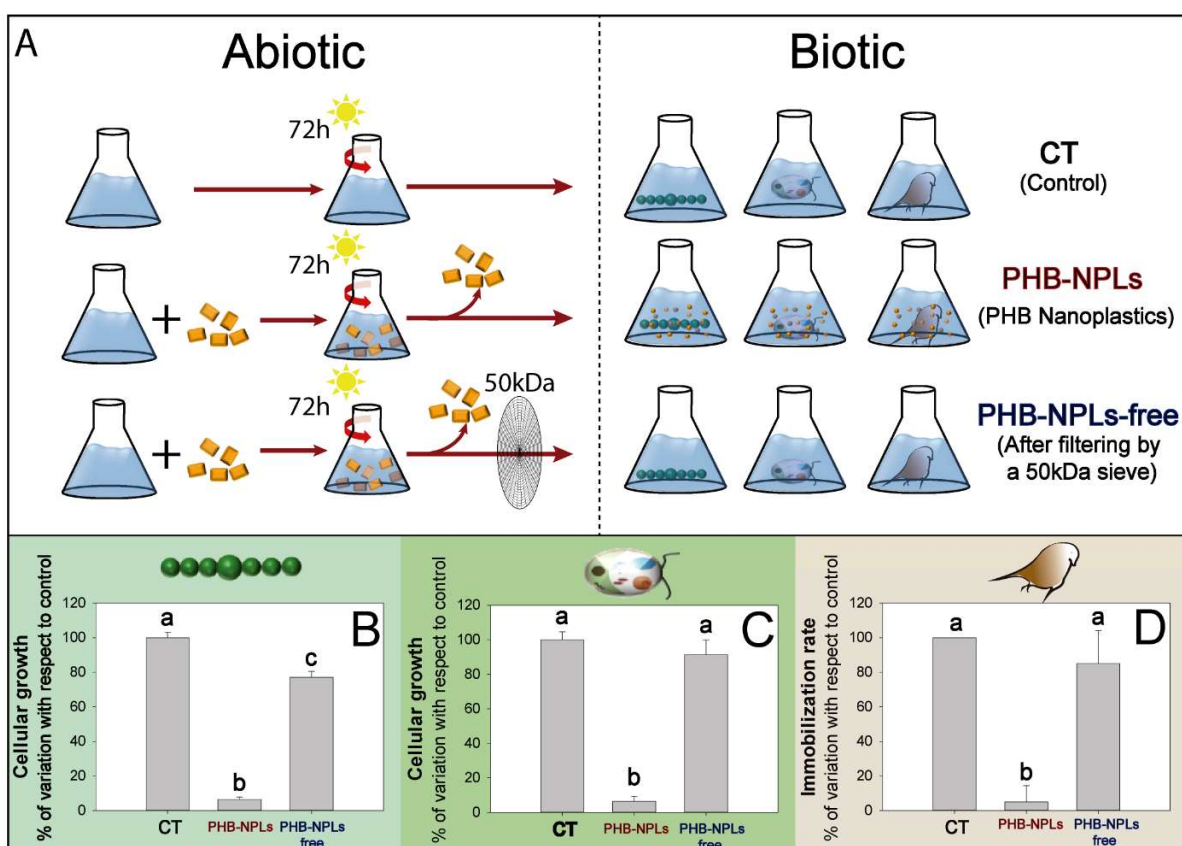


**Figure 2.** Effect of PHB-NPLs towards representative organisms of freshwater ecosystems. A) Experimental framework showing abiotic degradation in the appropriate culture medium to obtain PHB-NPLs (NPLs) and PHB-NPLs-free (NPLS-free) and biotic approaches to test the toxicity of PHB-NPLs are also shown. B), C) and D) Effect of PHB-NPLs and PHB-NPLs-free on cellular growth of *Anabaena* sp. PCC7120 (OD<sub>750nm</sub>) and *Chlamydomonas reinhardtii* (OD<sub>750nm</sub>) after 3 days of exposure and immobilization rate of *Daphnia magna* after 48 hours of exposure. Results are shown as percentage of variation of growth and immobilization rate  $\pm$  SD with respect to control. Letters indicate treatments that are significantly different to the control (Tukey's HSD,  $p < 0.001$ )

### The effects of PHB-NPLs towards aquatic organisms

After the extensive physicochemical characterization, the biological effect of the released PHB-NPLs was also tested and assessed by using two primary producers, the cyanobacterium *Anabaena* and the green alga *C. reinhardtii* and a primary consumer, the crustacean *D. magna*. These organisms play a key role in freshwater ecosystems. Cyanobacteria and algae (such as *Anabaena* and *C. reinhardtii*) are primary producers in freshwater ecosystems. They are involved in the carbon cycle, including global CO<sub>2</sub> sequestration. In addition, cyanobacteria are crucial in biogeochemical cycles, such as nitrogen and phosphorus cycles. Crustaceans (such as *D. magna*) are primary consumers. Changes affecting the primary producers and primary consumers may have detrimental effects on the entire ecosystem. Therefore, bioassays based on primary producers and consumers are pivotal to assess the risk of pollution to the biota in freshwater ecosystems. Following international standard bioassays, the three model aquatic organisms were exposed to the

released PHB-NPLs after 3 days of abiotic degradation (Fig. 2A). PHB-NPLs displayed a considerable toxic effect towards the three organisms. They significantly decreased the growth of both *Anabaena* (Fig. 2B) and *C. reinhardtii* (Fig. 2C) by 90 and 95%, respectively. Regarding *D. magna*, after 48 h of exposure, PHB-NPLs induced a significant immobilization (85%) of the organisms (Fig. 2D).

This detrimental effect could be due either to the PHB-NPLs themselves or to other abiotic degradation products released from PHB-microplastics. To check this, PHB-NPLs-free (see above) suspension was also tested. PHB-NPLs-free was non-toxic to *C. reinhardtii* (Fig. 2C) or *D. magna* (Fig. 2D) and a slight toxic effect was observed in the cyanobacterial growth (Fig. 2B). All these results indicated that the PHB-NPLs removed during the ultrafiltration step were responsible for the observed toxicity ruling out the presence of any toxic additive or chemical in the solution. In fact, the manufacturer claims that the main impurity is only bacterial cell wall debris (see Materials and Methods).



Moreover, dose-response bioassays were performed using dilutions of PHB-NPLs obtained after 3 days of abiotic degradation. The results showed a negative correlation since more diluted suspensions were less toxic than undiluted suspension, following a typical dose-response curve while increasing the concentration of a toxicant (Fig. S6 in the ESI). The  $EC_{50}$  values for the growth of *Anabaena* and *C. reinhardtii* and for the immobilization of *D. magna* were inferred from these curves (Fig. S8 in the ESI). The  $EC_{50}$  values of  $139.0 \pm 4.0$ ,  $54.6 \pm 2.1$  and  $106.7 \pm 4.3$  mg of PHB-NPLs  $L^{-1}$  were obtained for *Anabaena*, *C. reinhardtii* and *D. magna* respectively, showing that the green alga was more sensitive than the cyanobacterium and crustacean to the PHB-NPLs.

### Toxicity mechanisms of PHB-NPLs

Once the toxicity was clearly linked with the presence of PHB-NPLs, additional biological analyses were performed regarding their toxic mode-of-action. Fig. 3 shows the alterations in all these parameters after the exposure PHB-NPLs at the level of the  $EC_{50}$  (Fig. S8 in the ESI). A clear and significant (Tukey's HSD,  $p < 0.05$ ) increase of intracellular ROS levels was observed in all organisms when were exposed to the PHB-NPLs. The increase was higher in *Anabaena* than in the green alga, reaching an increment of 167% and 115%, respectively (Fig. 3). To check whether PHB-NPLs may impair membrane integrity, cells were stained with propidium iodide (PI; a frequently used fluorescence

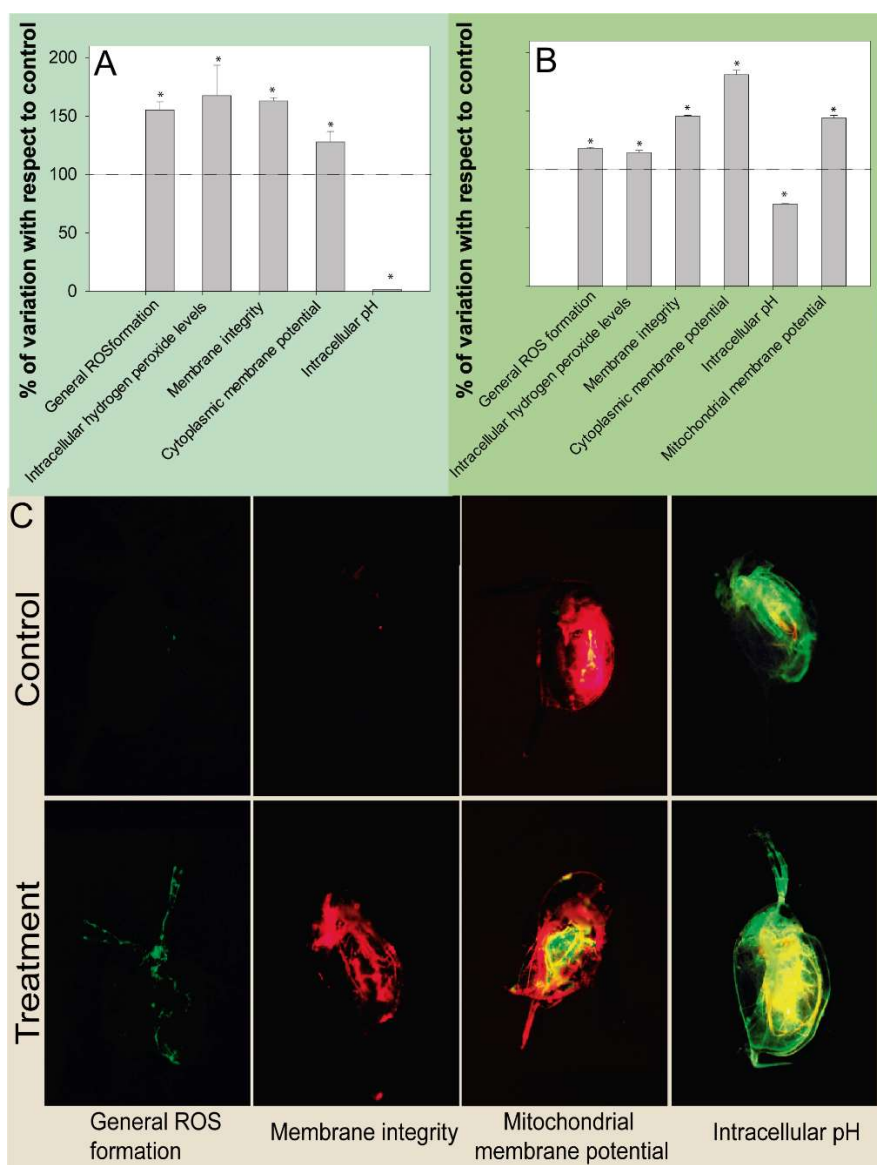


**Figure 3.** Toxicity mechanisms of PHB-NPLs in representative organisms of freshwater ecosystems. A), B) and C) alteration of relevant physiological parameters of *Anabaena* sp. PCC7120, *Chlamydomonas reinhardtii* after 3 days and *Daphnia magna* after 48 hours of exposure to PHB-NPLs. Results are shown as percentage of variation of relevant physiological parameters  $\pm$  SD with respect to control. Asterisk indicate treatments that are significantly different to the control (Dunnett's test,  $p < 0.05$ ).

indicator for membrane integrity). As can be observed in Fig 3, the fluorescence of PI was clearly increased after exposure to PHB-NPLs in the photosynthetic organisms (over 163% in *Anabaena* and around 146% in the alga) and crustacean as shown by confocal microscopy, indicating severe membrane damage. The impairment of membrane integrity might also increase non-specific permeability leading to membrane depolarization. Exposure to PHB-NPLs clearly altered cytoplasmic membrane potential, causing a strong depolarization of the membrane in both photosynthetic organisms (128% increase in *Anabaena* and 181% in the alga) and in *D. magna* as shown by confocal microscopy. Moreover, in the alga and crustacean, PHB-NPLs exposure resulted in a significant (Tukey's HSD,  $p < 0.05$ ) mitochondrial membrane potential depolarization (Fig. 3). In summary, mechanistic studies revealed that PHB-NPLs increased ROS formation, which subsequently damaged cytoplasmic membrane integrity and altered its permeability. In the case of the alga and the crustacean, this may end in mitochondrial performance impairment. Eventually, all these alterations may result in growth inhibition or death of the three freshwater organisms.

## Discussion

A major challenge in understanding environmental impact of plastics on ecosystems is to know whether secondary nanoplastics formed under environmentally representative conditions can exert a toxic effect. Our study offers a fine-grained perspective on how secondary nanoplastics released from microplastics are responsible for the observed toxicity towards relevant freshwater organisms. This study has especially focused on biodegradable plastics such as PHB, since biodegradable plastics are considered the best candidates to replace the non-biodegradable ones.

Our results indicate that PHB-NPLs are produced quickly during abiotic degradation under environmentally representative conditions from PHB-microplastics. The release of nanoplastic particles is faster than thought as the results presented here showed PHB-NPLs formation after only three days of abiotic degradation versus the longer previous times which were previously reported for other plastics<sup>17-19</sup>. Factors like their micrometric size and biodegradability could explain the higher amount of nanoplastics released from PHB unlike previous studies. Moreover, the biological effects of these degradation products have not been assessed until date. Taking into account the results revealed here, biodegradable plastics may not be safe for freshwater organisms. Therefore, precautionary measures should be taken before replacing the non-biodegradable plastics by biodegradable ones such as PHB. PHB-NPLs induced a significant decrease in

cellular growth and altered relevant physiological parameters in the three tested organisms. Our results are in agreement with several studies which show that nanoplastics exert toxic effects towards aquatic organisms<sup>2, 10, 21, 22, 36, 37</sup>. However, those studies are based on primary nanoparticles with a well-defined structure and size distribution which may not reflect the environmental conditions. Nevertheless, compared with previous studies, the effect based on EC<sub>50</sub> values showed that, in general, PHB-NPLs are more toxic than primary nanoplastics for crustacean as well as for other photosynthetic organisms<sup>2, 10, 21, 22, 36, 37</sup>. It should be taken into account that our work is the first clearly showing the toxic effect of secondary nanoplastics formed as by-product of a biodegradable microplastic under environmentally representative conditions towards freshwater organisms of different trophic levels (cyanobacteria, algae and crustacean), which showed similar physiological responses to PHB-NPLs, such as ROS formation, which is a common response to nanoparticles, that affects lipids and proteins eventually leading to damage of the cytoplasmic membrane and compromising its integrity<sup>38, 39</sup>. In such context, increasing evidence indicates that primary nanoplastics in general can also induce ROS overproduction that can damage cell membrane integrity leading to apoptosis<sup>40, 41</sup>. Our results also offer an alternative explanation to the emergence of toxic effects of leachates from virgin plastics and microplastics in which the concentrations of released chemicals (or their mixture) are usually several orders of magnitude lower than the effective concentration of those chemicals that might cause toxicity or unknown<sup>42-45</sup>, highlighting the importance of secondary nanoplastics in the toxicity of plastics. The current belief that biodegradable plastics are safer for the environment should be revisited in order to accomplish an adequate environmental health and safety assessment of plastics.

## Conclusions

Secondary PHB-nanoplastics were released from PHB-microplastics by abiotic degradation under environmentally representative conditions. These were harmful for three freshwater organisms that play a key role in freshwater ecosystems. All results put together indicated that biodegradable plastic does not mean safe for the environment in the case of PHB. Future studies on plastic ecotoxicity should focus on secondary nanoplastics formed as a consequence of degradation of plastics.

## Acknowledgements

We thank Malvern for the Nanoparticle Tracking Analysis. This research was supported by the Spanish Ministerio de Economía y Competitividad, grants CTM2016-74927-C2-1/2-R. MGP thanks the Comunidad de Madrid – EU for the award of a postdoctoral grant (Postdoc FSE-YEI). MTB

thanks the Spanish Ministerio de Educación y Formación Profesional for the award of a pre-doctoral grant (FPU). GA, thanks the Universidad de Alcalá for the award of a pre-doctoral grant (FPI-UAH).

## References

1. The future of plastic, *Nat Commun*, 2018, **9**, 2157.
2. J. P. da Costa, P. S. Santos, A. C. Duarte and T. Rocha-Santos, (Nano) plastics in the environment—sources, fates and effects, *Science of the Total Environment*, 2016, **566**, 15-26.
3. J. Gigault, A. Ter Halle, M. Baudrimont, P.-Y. Pascal, F. Gauffre, T.-L. Phi, H. El Hadri, B. Grassl and S. Reynaud, Current opinion: What is a nanoplastic?, *Environmental Pollution*, 2018, **235**, 1030-1034.
4. S. K. Kale, A. G. Deshmukh, M. S. Dudhare and V. B. Patil, Microbial degradation of plastic: a review, *Journal of Biochemical Technology*, 2015, **6**, 952-961.
5. P. Europe, Plastics – the Facts 2017, An analysis of European plastics production, demand and waste data. *Journal*, 2017.
6. M. Rujnić-Sokele and A. Pilipović, Challenges and opportunities of biodegradable plastics: A mini review, *Waste Management & Research*, 2017, **35**, 132-140.
7. R. T. Chan, C. J. Garvey, H. Marçal, R. A. Russell, P. J. Holden and L. J. R. Foster, Manipulation of polyhydroxybutyrate properties through blending with ethyl-cellulose for a composite biomaterial, *International Journal of Polymer Science*, 2011, **2011**.
8. S. Lambert and M. Wagner, in *Freshwater Microplastics : Emerging Environmental Contaminants?*, eds. M. Wagner and S. Lambert, Springer International Publishing, Cham, 2018, DOI: 10.1007/978-3-319-61615-5\_1, pp. 1-23.
9. W. Li, H. Tse and L. Fok, Plastic waste in the marine environment: A review of sources, occurrence and effects, *Science of the Total Environment*, 2016, **566**, 333-349.
10. K. Mattsson, S. Jovic, I. Doverbratt and L.-A. Hansson, in *Microplastic Contamination in Aquatic Environments*, Elsevier, 2018, pp. 379-399.
11. S. Lambert, C. Sinclair and A. Boxall, in *Reviews of Environmental Contamination and Toxicology, Volume 227*, Springer, 2014, pp. 1-53.
12. J. P. Harrison, T. J. Hoellein, M. Sapp, A. S. Tagg, Y. Ju-Nam and J. J. Ojeda, in *Freshwater Microplastics : Emerging Environmental Contaminants?*, eds. M. Wagner and S. Lambert, Springer International Publishing, Cham, 2018, DOI: 10.1007/978-3-319-61615-5\_9, pp. 181-201.
13. S. Klein, I. K. Dimzon, J. Eubeler and T. P. Knepper, in *Freshwater Microplastics : Emerging Environmental Contaminants?*, eds. M. Wagner and S. Lambert, Springer International Publishing, Cham, 2018, DOI: 10.1007/978-3-319-61615-5\_3, pp. 51-67.
14. NOAA, Proceedings of the International Research Workshop on the Occurrence, Effects, and Fate of Microplastic Marine Debris, September 9-11, 2008, NOAA Technical Memorandum NOS-OR&R-30, National Oceanic and Atmospheric Administration Marine Debris Program, U.S. Department of Commerce, 2009.
15. J. Li, H. Liu and J. P. Chen, Microplastics in freshwater systems: A review on occurrence, environmental effects, and methods for microplastics detection, *Water research*, 2018, **137**, 362-374.
16. J. Gigault, B. Pedrono, B. Maxit and A. Ter Halle, Marine plastic litter: the unanalyzed nano-fraction, *Environmental Science: Nano*, 2016, **3**, 346-350.
17. S. Lambert, C. J. Sinclair, E. L. Bradley and A. B. Boxall, Effects of environmental conditions on latex degradation in aquatic systems, *Science of the total environment*, 2013, **447**, 225-234.
18. S. Lambert and M. Wagner, Formation of microscopic particles during the degradation of different polymers, *Chemosphere*, 2016, **161**, 510-517.
19. S. Lambert and M. Wagner, Characterisation of nanoplastics during the degradation of polystyrene, *Chemosphere*, 2016, **145**, 265-268.
20. L. M. Hernandez, N. Yousefi and N. Tufenkji, Are there nanoplastics in your personal care products?, *Environmental Science & Technology Letters*, 2017, **4**, 280-285.
21. Y. Chae and Y.-J. An, Effects of micro- and nanoplastics on aquatic ecosystems: Current research trends and perspectives, *Marine pollution bulletin*, 2017, **124**, 624-632.
22. S. M. Harmon, in *Microplastic Contamination in Aquatic Environments*, Elsevier, 2018, pp. 249-270.
23. N. Corcoll, B. Bonet, M. Leira, B. Montuelle, A. Tlili and H. Guasch, Light history influences the response of fluvial biofilms to Zn exposure, *Journal of phycology*, 2012, **48**, 1411-1423.
24. S. Gonzalo, I. Rodea-Palomares, F. Leganés, E. García-Calvo, R. Rosal and F. Fernández-Piñas, First evidences of PAMAM dendrimer internalization in microorganisms of environmental relevance: a linkage with toxicity and oxidative stress, *Nanotoxicology*, 2015, **9**, 706-718.
25. R. Rosal, I. Rodea-Palomares, K. Boltes, F. Fernández-Piñas, F. Leganés and A. Petre, Ecotoxicological assessment of surfactants in the aquatic environment: combined toxicity of docusate sodium with chlorinated pollutants, *Chemosphere*, 2010, **81**, 288-293.
26. R. Prado, C. Rioboo, C. Herrero and Á. Cid, Screening acute cytotoxicity biomarkers using a microalga as test organism, *Ecotoxicology and environmental safety*, 2012, **86**, 219-226.
27. M. T. Belda, M. Gonzalez-Pleiter, G. Pulido-Reyes, K. Martin-betancor, F. Leganes, R. Rosal and F. Fernandez-Piñas, Mechanism of toxic action of cationic G5 and G7 PAMAM dendrimers in the cyanobacterium *Anabaena* sp. PCC7120, *Environmental Science: Nano*, 2019.
28. R. J. Paul, M. Colmorgen, R. Pirow, Y.-H. Chen and M.-C. Tsai, Systemic and metabolic responses in *Daphnia magna* to anoxia, *Comparative Biochemistry and Physiology Part A: Molecular & Integrative Physiology*, 1998, **120**, 519-530.
29. V. V. Teplova, Z. I. Andreeva-Kovalevskaya, E. V. Sineva and A. S. Solonin, Quick assessment of cytotoxins effect on *Daphnia magna* using in vivo

- fluorescence microscopy, *Environmental toxicology and chemistry*, 2010, **29**, 1345-1348.
30. J. Liu and W.-X. Wang, The protective roles of TiO<sub>2</sub> nanoparticles against UV-B toxicity in *Daphnia magna*, *Science of the Total Environment*, 2017, **593**, 47-53.
  31. M. Ramezani, M. Amoozegar and A. Ventosa, *Screening and comparative assay of poly-hydroxyalkanoates produced by bacteria isolated from the Gavkhooni Wetland in Iran and evaluation of poly-β-hydroxybutyrate production by halotolerant bacterium Oceanimonas sp. GK1*, 2014.
  32. H. P. Erickson, Size and shape of protein molecules at the nanometer level determined by sedimentation, gel filtration, and electron microscopy, *Biological procedures online*, 2009, **11**, 32.
  33. P. Anbukarasu, D. Sauvageau and A. Elias, Tuning the properties of polyhydroxybutyrate films using acetic acid via solvent casting, *Scientific reports*, 2015, **5**, 17884.
  34. A. Bonartsev, A. Boskhomodgiev, A. Iordanskii, G. Bonartseva, A. Rebrov, T. Makhina, V. Myshkina, S. Yakovlev, E. Filatova and E. Ivanov, Hydrolytic degradation of poly (3-hydroxybutyrate), polylactide and their derivatives: kinetics, crystallinity, and surface morphology, *Molecular Crystals and Liquid Crystals*, 2012, **556**, 288-300.
  35. M. Hakkarainen, in *Degradable aliphatic polyesters*, Springer, 2002, pp. 113-138.
  36. S. Rist and N. B. Hartmann, in *Freshwater Microplastics : Emerging Environmental Contaminants?*, eds. M. Wagner and S. Lambert, Springer International Publishing, Cham, 2018, DOI: 10.1007/978-3-319-61615-5\_2, pp. 25-49.
  37. J.-K. Wan, W.-L. Chu, Y.-Y. Kok and C.-S. Lee, Distribution of Microplastics and Nanoplastics in Aquatic Ecosystems and Their Impacts on Aquatic Organisms, with Emphasis on Microalgae, 2018.
  38. P. Khanna, C. Ong, B. Bay and G. Baeg, Nanotoxicity: an interplay of oxidative stress, inflammation and cell death, *Nanomaterials*, 2015, **5**, 1163-1180.
  39. T. Suman, S. R. Rajasree and R. Kirubakaran, Evaluation of zinc oxide nanoparticles toxicity on marine algae *Chlorella vulgaris* through flow cytometric, cytotoxicity and oxidative stress analysis, *Ecotoxicology and environmental safety*, 2015, **113**, 23-30.
  40. L. Canesi, C. Ciacchi, E. Bergami, M. Monopoli, K. Dawson, S. Papa, B. Canonico and I. Corsi, Evidence for immunomodulation and apoptotic processes induced by cationic polystyrene nanoparticles in the hemocytes of the marine bivalve *Mytilus*, *Marine environmental research*, 2015, **111**, 34-40.
  41. Z. Liu, M. Cai, P. Yu, M. Chen, D. Wu, M. Zhang and Y. Zhao, Age-dependent survival, stress defense, and AMPK in *Daphnia pulex* after short-term exposure to a polystyrene nanoplastic, *Aquatic Toxicology*, 2018, **204**, 1-8.
  42. E. S. P. P. Gandara, C. R. Nobre, P. Resaffe, C. D. S. Pereira and F. Gusmao, Leachate from microplastics impairs larval development in brown mussels, *Water Res*, 2016, **106**, 364-370.
  43. C. Martinez-Gomez, V. M. Leon, S. Calles, M. Gomariz-Olcina and A. D. Vethaak, The adverse effects of virgin microplastics on the fertilization and larval development of sea urchins, *Marine environmental research*, 2017, **130**, 69-76.
  44. M. S. Taylor, A. U. Daniels, K. P. Andriano and J. Heller, Six bioabsorbable polymers: in vitro acute toxicity of accumulated degradation products, *J Appl Biomater*, 1994, **5**, 151-157.
  45. C. Thaysen, K. Stevack, R. Ruffolo, D. Poirier, H. De Frond, J. DeVera, G. Sheng and C. M. Rochman, Leachate From Expanded Polystyrene Cups Is Toxic to Aquatic Invertebrates (*Ceriodaphnia dubia*), *Frontiers in Marine Science*, 2018, **5**.

## SUPPLEMENTARY MATERIAL

### Secondary nanoplastics released from a biodegradable microplastic severely impact freshwater environments

Miguel González-Pleiter<sup>1,\*</sup>, Miguel Tamayo-Belda<sup>1</sup>, Gerardo Pulido-Reyes<sup>1</sup>, Georgiana Amariei<sup>2</sup>, Francisco Leganés<sup>1</sup>, Roberto Rosal<sup>2</sup> and Francisca Fernández-Piñas<sup>1</sup>

<sup>1</sup> Department of Biology, Faculty of Science, Universidad Autónoma de Madrid, Spain

<sup>2</sup> Department of Chemical Engineering, Universidad de Alcalá, E-28871 Alcalá de Henares, Spain

\* Corresponding author: mig.gonzalez@uam.es

#### Contents:

**Figure S1.** SEM images of surface smoothing of PHB-microplastics abiotically degraded in Milli-Q water buffered with 2 mM phosphate (pH 7.0) at 28 °C in constant shaking (135 rpm) during: 0 days (A-E), 3 days (F-J) and 20 days (K-O) and at 3 different magnifications (74x, 3000x and 25000x; scale bars included). At higher magnifications white arrows indicate representative structures of the smoothing process at each degradation time, in both the micrometric range, studied at 3000x (B, C, G, H, L and M), and the nanometric range, studied at 25000x (D, E, I, J, N and O).

**Figure S2.** ATR-FTIR of PHB-microplastics before and after 3 days of abiotic degradation.

**Figure S3.** Concentration of secondary PHB-nanoplastics released from different initial concentration of PHB-microplastics (25, 50 and 100 mg/L) after 3 days of abiotic degradation.

**Figure S4.** Physicochemical characterization of the PHB-nanoplastics suspension (obtained from the supernatant of 50 mg/ml of PHB-microplastics abiotically degraded in Milli-Q water buffered with 2 mM phosphate (pH 7.0) at 28 °C in constant shaking for 3 days) before and after ultrafiltration by 50 KDa MWCO (pore size of approximately 4 nm). The amount of particulate matter removed by ultrafiltration was measured by comparing the total organic carbon (TOC) before and after the ultrafiltration and was expressed as the percentage that remains in the ultrafiltrated solution with respect to the non-ultrafiltrated one (A). Size distribution by DLS was also analysed before ultrafiltration (B), displaying a size of around 200 nm (done by triplicate), and after the ultrafiltration (C) showing a size less than 1 nm, essentially equal to that observed after ultrafiltration of the Milli-Q water buffered with 2mM of phosphate (pH 7.0).

**Figure S5.** The total number of formed PHB-NPLs per unit mass of PHB-microplastic after 3 days of abiotic degradation measured by NTA.

**Figure S6.** NTA size distribution of PHB-NPLs obtained from different initial concentration of PHB-microplastics (25, 50 and 100 mg/L) after 3 days of abiotic degradation. Milli-Q blank signal was subtracted from the samples.

**Figure S7.** Secondary PHB nanoplastics released from PHB microplastics (50 mg/mL) after 3 days of the abiotic degradation process under light (ca. 65  $\mu\text{mol photons m}^{-2} \text{s}^{-1}$ ) and dark. No significant differences were found.

**Figure S8.** Dose-response curves of increasing PHB-NPLs concentrations on cellular growth ( $\text{OD}_{750\text{nm}}$ ) of *Anabaena* sp. PCC7120 (A) and *Chlamydomonas reinhardtii* (B) cells and immobilization rate of *Daphnia magna* (C) after 3 days of exposure. Results are shown as percentage of variation of growth or immobilization rate  $\pm$  SD with respect to controls.

**Table S1.** Properties of the polyhydroxybutyrate monomer

**Table S2.** Fluorochromes used to evaluate the physiological parameters.

**Table S3.** DLS diameter and  $\zeta$ -potential of PHB-NPLs particles released in the abiotic degradation experiment from different initial concentration of PHB-microplastics after 3 days.



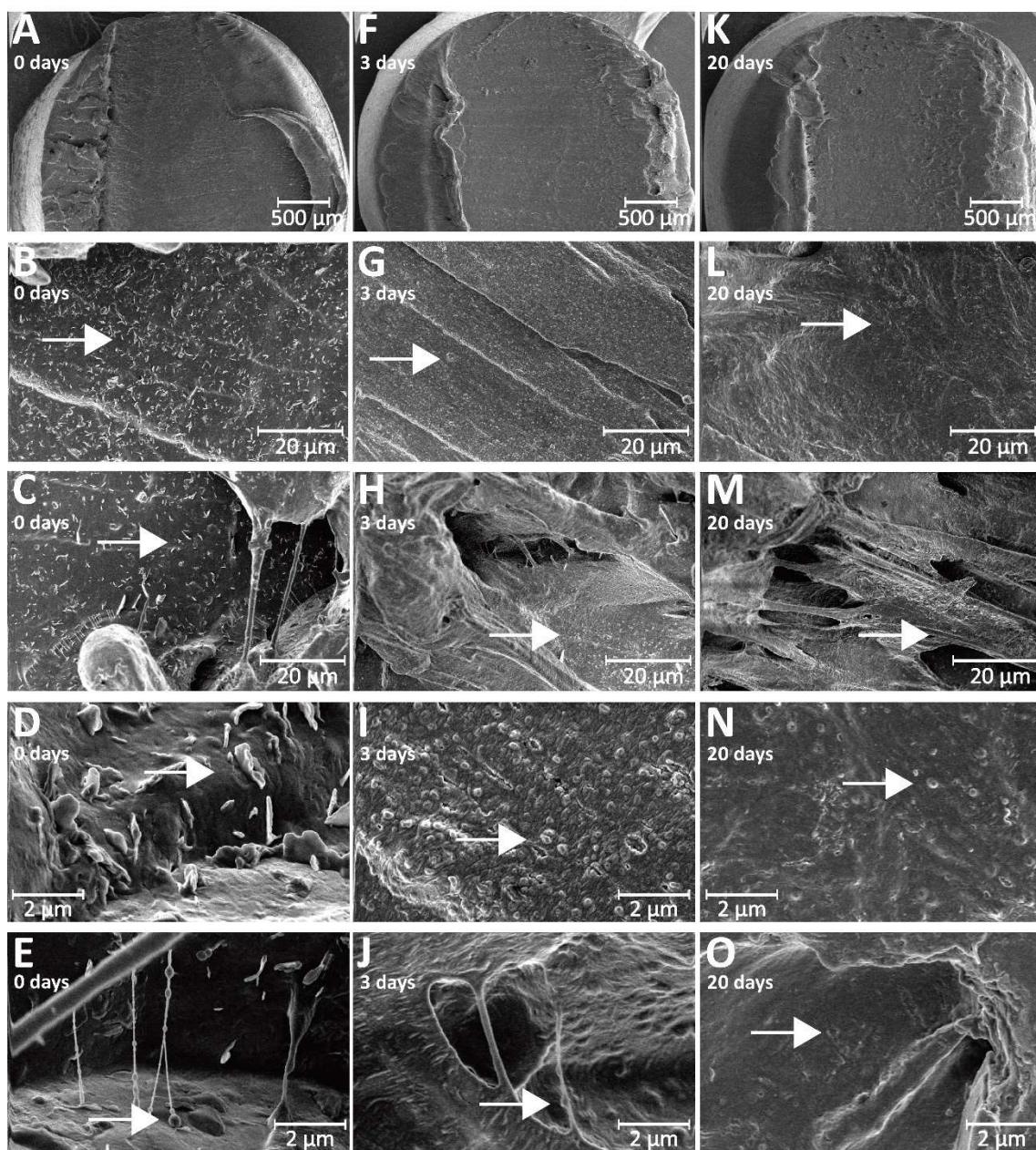


**Figure S1.** SEM images of surface smoothing of PHB-microplastics abiotically degraded in Milli-Q water buffered with 2 mM phosphate (pH 7.0) at 28 °C in constant shaking (135 rpm) during: 0 days (A-E), 3 days (F-J) and 20 days (K-O) and at 3 different magnifications (74x, 3000x and 25000x; scale bars included). At higher magnifications white arrows indicate representative structures of the smoothing process at each degradation time, in both the micrometric range, studied at 3000x (B, C, G, H, L and M), and the nanometric range, studied at 25000x (D, E, I, J, N and O).



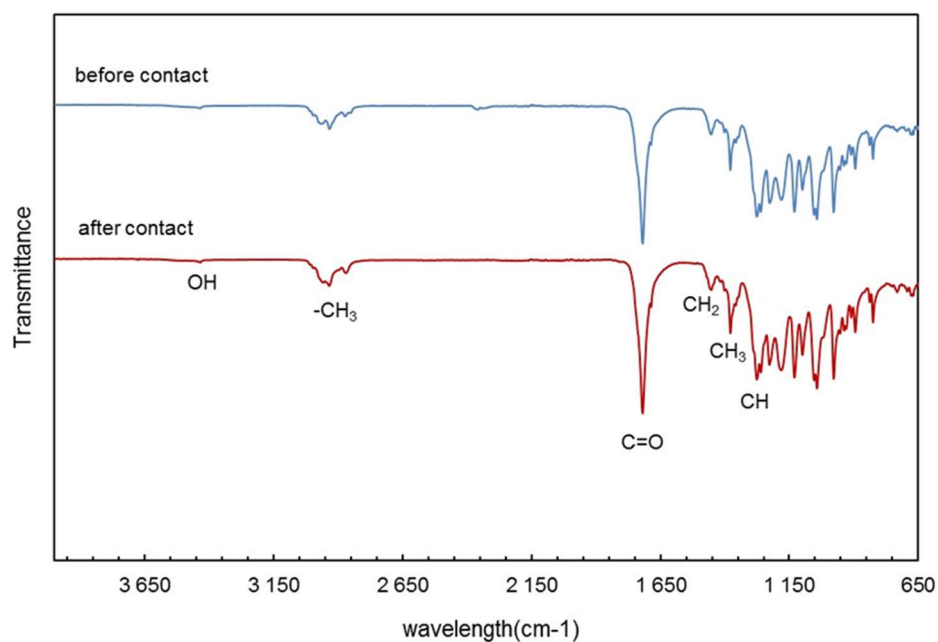


**Figure S2.** ATR-FTIR of PHB-microplastics before and after 3 days of abiotic degradation.

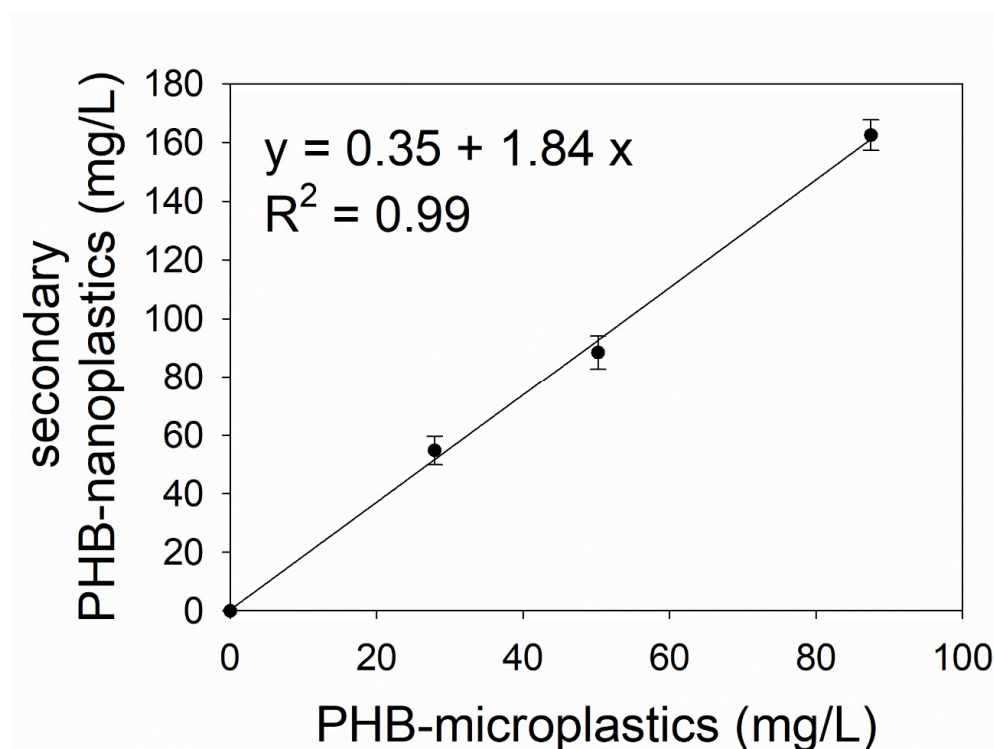


**Figure S3.** Concentration of secondary PHB-nanoplastics released from different initial concentration of PHB-microplastics (25, 50 and 100 mg/L) after 3 days of abiotic degradation.

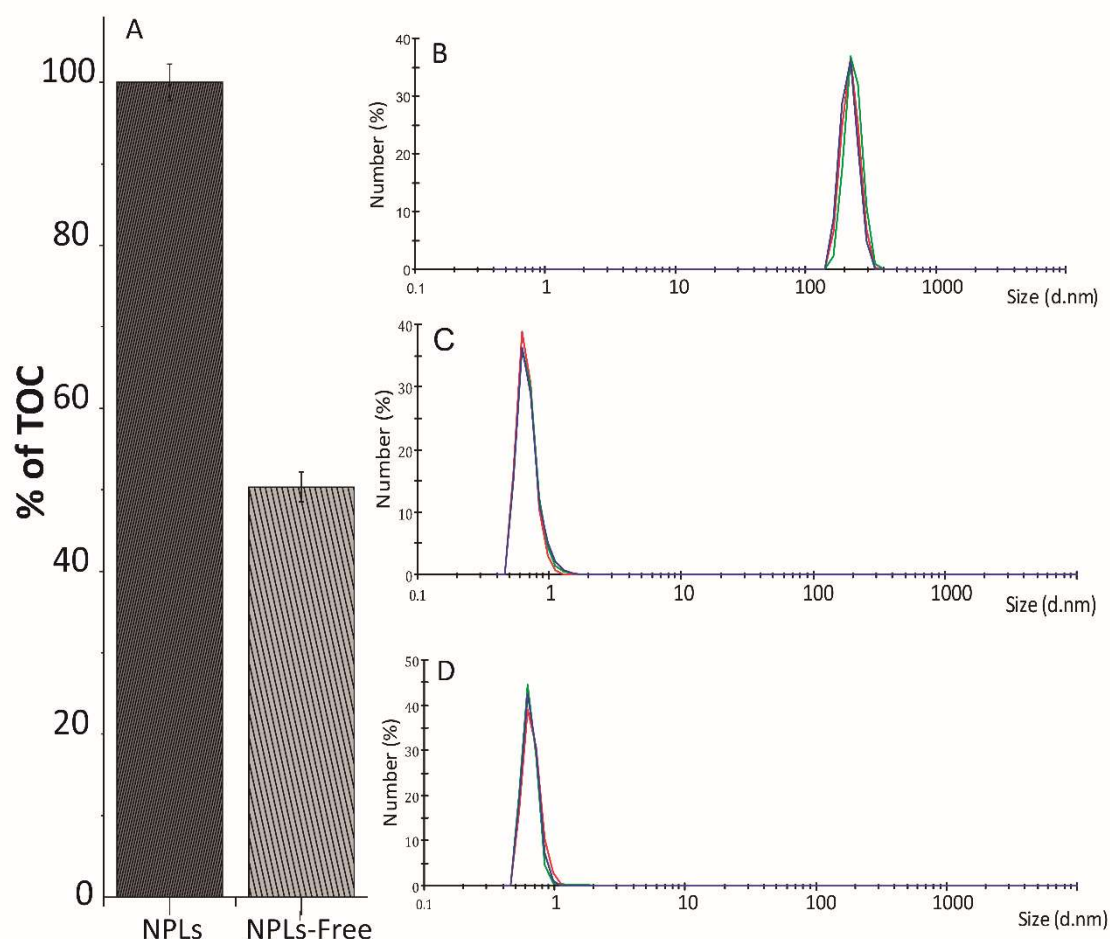


**Figure S4.** Physicochemical characterization of the PHB-nanoplastics suspension (obtained from the supernatant of 50 mg/ml of PHB-microplastics abiotically degraded in Milli-Q water buffered with 2 mM phosphate (pH 7.0) at 28 °C in constant shaking for 3 days) before and after ultrafiltration by 50 KDa MWCO (pore size of approximately 4 nm). The amount of particulate matter removed by ultrafiltration was measured by comparing the total organic carbon (TOC) before and after the ultrafiltration and was expressed as the percentage that remains in the ultrafiltrated solution with respect to the non-ultrafiltrated one (A). Size distribution by DLS was also analysed before ultrafiltration (B), displaying a size of around 200 nm (done by triplicate), and after the ultrafiltration (C) showing a size less than 1 nm, essentially equal to that observed after ultrafiltration of the Milli-Q water buffered with 2mM of phosphate (pH 7.0).

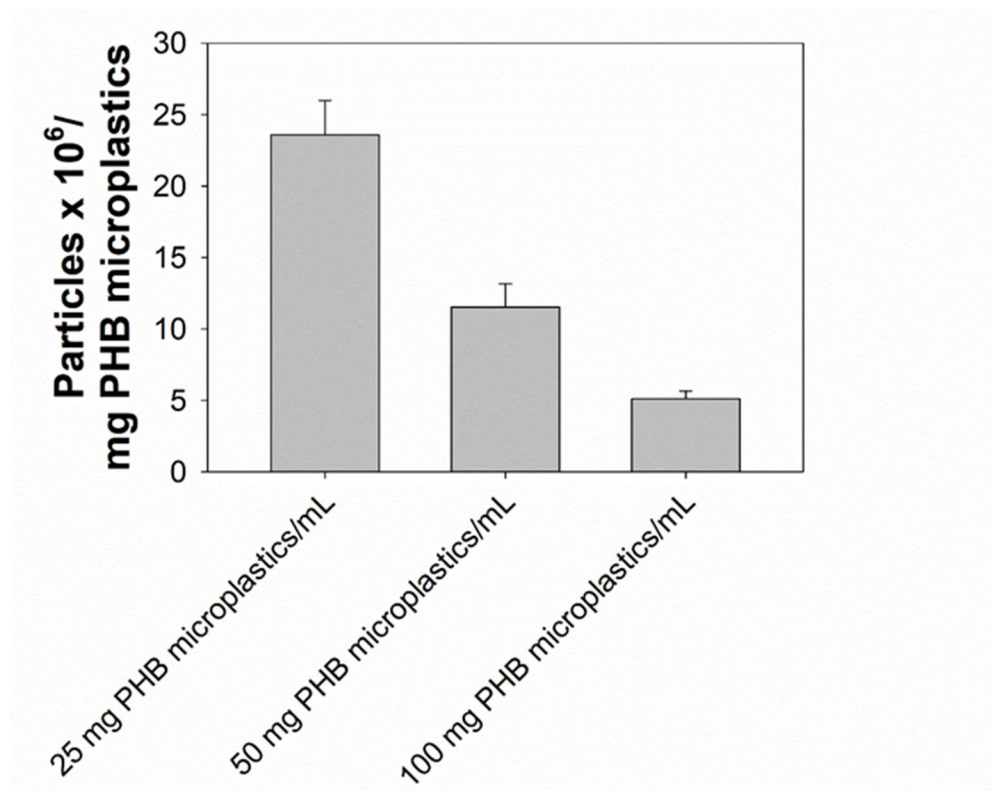


**Figure S5.** The total number of formed PHB-NPLs per unit mass of PHB-microplastic after 3 days of abiotic degradation measured by NTA.

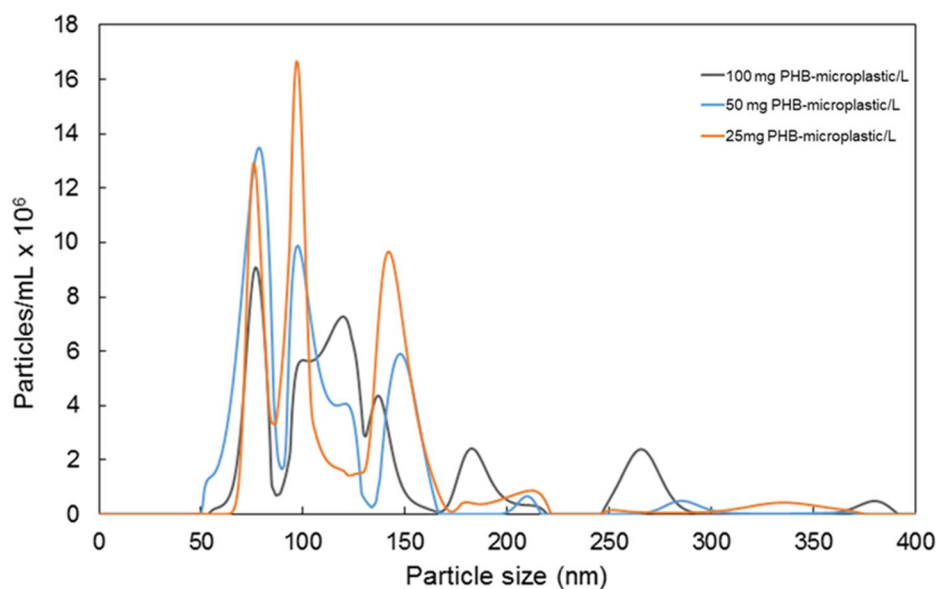


**Figure S6.** NTA size distribution of PHB-NPLs obtained from different initial concentration of PHB-microplastics (25, 50 and 100 mg/L) after 3 days of abiotic degradation. Milli-Q blank signal was subtracted from the samples.

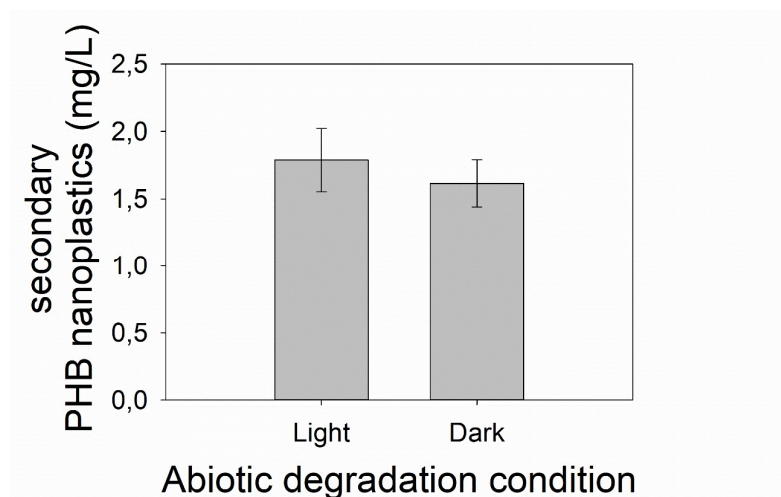


**Figure S7.** Secondary PHB nanoplastics released from PHB microplastics (50 mg/mL) after 3 days of the abiotic degradation process under light (ca. 65  $\mu\text{mol photons m}^{-2} \text{s}^{-1}$ ) and dark. No significant differences were found.

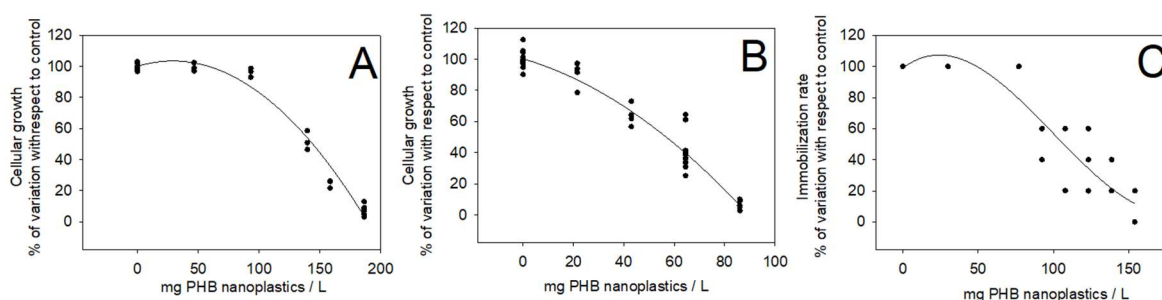


**Figure S8.** Dose-response curves of increasing PHB-NPLs concentrations on cellular growth (OD<sub>750nm</sub>) of *Anabaena* sp. PCC7120 (A) and *Chlamydomonas reinhardtii* (B) cells and immobilization rate of *Daphnia magna* (C) after 3 days of exposure. Results are shown as percentage of variation of growth or immobilization rate  $\pm$  SD with respect to controls.

**Table S1.** Properties of the polyhydroxybutyrate monomer

| Polyhydroxybutyrate (PHB)  |   |
|--|---|
| Molecular weight   | 86 g/mol  |
| Formula  | C <sub>4</sub> H <sub>6</sub> O <sub>2</sub>  |
| Chemical structure   | $\left[ \text{CH}_2 - \text{CH}(\text{CH}_3) - \text{CH}_2 - \text{C}(=\text{O})\text{O} \right]_n$   |
| Estimation of the PHB-nanoplastics concentration using the ratio: C per PHB molecule | The mg of PHB nanoplastics per L were calculated from mg of TOC using the ratio of C per PHB molecule: $(12 \text{ u} \times 4\text{C}) / ((12 \text{ u} \times 4\text{C}) + (1 \text{ u} \times 6\text{H}) + (16 \text{ u} \times 2\text{O})) = 0.558 \text{ mg of C per mg of PHB}$ . Despising the functional groups that could appear after the production of PHB-nanoplastics from PHB-microplastics |

**Table S2.** Fluorochromes used to evaluate the physiological parameters.

| Fluorochrome           | Applications                              | Mode of action  | Final concentration<br><i>Anabaena</i> sp.<br>PCC7120 | Final concentration<br><i>Chlamydomonas</i><br><i>reinhardtii</i> | Final concentration<br><i>Daphnia magna</i> |
|------------------------|---|---|---|---|---|
| DCFH                   | General ROS                               | DCFH is a chemical indicator that diffuses freely into the cells. Once that it enters the cell, esterases cleave the ester bond and turns to highly fluorescent 2',7'-dichlorofluorescein upon oxidation. Therefore, DCFH are used to detect oxidative products in cells. (recorded in FL1 channel)   | 100 $\mu$ M   | 50 $\mu$ M  | 100 $\mu$ M                                 |
| DHR123                 | Intracellular levels of hydrogen peroxide | DHR123 passively diffuses across cell membranes. Once that it enters the cell, it can be oxidized, mainly by H <sub>2</sub> O <sub>2</sub> , in a slow reaction unless catalysed by an enzyme with peroxidase activity, and secondarily by peroxynitrite anion, to form cationic rhodamine 123. This is a fluorescent compound which localizes in the mitochondria emitting a bright fluorescent signal (recorded in FL1 channel)   | 10 $\mu$ g/mL   | 10 $\mu$ g/mL   | -   |
| PI                     | Membrane integrity                        | Due to its polarity, PI is unable to pass through intact cell membranes. However, when the integrity of the cell membranes is damaged, PI is able to enter and to intercalate with double-stranded nucleic acids to produce red fluorescence (recorded in FL3 channel)  | 5 $\mu$ g/mL  | 2.5 $\mu$ g/mL  | 10 $\mu$ g/mL                               |
| DiBAC <sub>4</sub> (3) | Cytoplasmic membrane potential            | DiBAC <sub>4</sub> (3) is lipophilic and shows high fluorescence dynamics upon changes in membrane potential by its Nernstian distribution between the inner and outer medium of the cells. Once the cells are equilibrated with DiBAC <sub>4</sub> (3), depolarization increases fluorescence (recorded in FL1 channel) when is the cells are excited with blue light (488nm excitation laser) as the negatively charged oxonol moves into the cells, where it is bound to intracellular proteins and membranes. Hyperpolarization decreases fluorescence (recorded in FL1 channel). Due to their overall negative charge, it is excluded from the mitochondria, so the mitochondrial membrane potential do not interfere the cytoplasmic membrane potential | 2.5 $\mu$ g/mL  | 0.5 $\mu$ g/mL  | -   |
| BCECF                  | Intracellular pH                          | BCECF-AM AM diffuses through the cell membrane and intracellular esterases cleave the ester bond, releasing BCECF. When BCECF AM is excited by blue light (488nm excitation laser), this fluorochrome emits fluorescence with a maximum at 525 nm. In the range of physiological pH, the emission intensity increases with increasing pH. The fluorescence emitted at 620 nm is not pH-dependent. In spite of this wavelength, it is not really an isosbestic point. The ratio of fluorescence emitted at 525 and 620 nm (green/red) was used to analyse pH <sub>i</sub> in cells stained with BCECF  | 5 $\mu$ g/mL  | 5 $\mu$ g/mL  | 10 $\mu$ g/mL                               |
| JC-1                   | Mitochondrial membrane potential          | JC-1 exhibits potential-dependent accumulation in mitochondria and owns dual emission potential-sensitive. Fluorescence emission shifts from green (recorded in FL1 channel) to red (recorded in FL2 channel). Mitochondrial depolarization decreases the red/green fluorescence intensity ratio  | -   | 5 $\mu$ g/mL  | 40 $\mu$ g/mL                               |

**Table S3.** DLS diameter and  $\zeta$ -potential of PHB-NPLs particles released in the abiotic degradation experiment from different initial concentration of PHB-microplastics after 3 days.

| <b>Initial concentration of PHB-microplastics</b> | <b>25 mg PHB microplastics / mL</b> | <b>50 mg PHB microplastics / mL</b> | <b>100 mg PHB microplastics / mL</b> |
|---|-------------------------------------|-------------------------------------|--------------------------------------|
| DLS diameter (nm)                                 | 209 $\pm$ 17                        | 204 $\pm$ 22                        | 225 $\pm$ 37                         |
| $\zeta$ -potential at pH 7.0 (mV)                 | -19.1 $\pm$ 2.3                     | -19.7 $\pm$ 3.4                     | -20.7 $\pm$ 3.4                      |